Spectroscopy of Pionic Atoms in ^{122}Sn(d,^{3}He) Reaction and Angular Dependence of the Formation Cross Sections

T. Nishi *et al.* (piAF Collaboration)

Phys. Rev. Lett. **120**, 152505 — Published 13 April 2018

DOI: 10.1103/PhysRevLett.120.152505

Spectroscopy of pionic atoms in ^{122}Sn$(d,{}^3$He$)$ reaction and angular dependence of the formation cross sections

T. Nishi[1,2], K. Itahashi[2,*] G.P.A. Berg[3], H. Fujioka[4], N. Fukuda[2], N. Fukunishi[2], H. Geissel[5], R.S. Hayano[1], S. Hirenzaki[6], K. Ichikawa[1], N. Ikeno[7], N. Inabe[2], S. Itoh[1], M. Iwasaki[2], D. Kameda[2], S. Kawase[8], T. Kubo[2], K. Kusaka[2], H. Matsubara[8], S. Michimasa[8], K. Miki[1], G. Mishima[1], H. Miya[2], H. Nagahiro[6], M. Nakamura[2], S. Noji[1], K. Okochi[1], S. Ota[8], N. Sakamoto[2], K. Suzuki[9], H. Takeda[2], Y.K. Tanaka[1], K. Todoroki[1], K. Tsukada[2], T. Uesaka[2], Y.N. Watanabe[1], H. Weick[5], H. Yamakami[4], and K. Yoshida[2]

[1] *Department of Physics, School of Science, The University of Tokyo, 7-3-1 Hongo, Bunkyo-ku, 113-0033 Tokyo, Japan*

[2] *Nishina Center for Accelerator-Based Science, RIKEN, 2-1 Hirosawa, Wako, 351-0198 Saitama, Japan*

[3] *Department of Physics and the Joint Institute for Nuclear Astrophysics Center for the Evolution of the Elements, University of Notre Dame, Notre Dame, Indiana 46556, USA*

[4] *Department of Physics, Kyoto University, Kitashirakawa-Oiwakecho, Sakyo-ku, Kyoto, 606-8502 Kyoto, Japan*

[5] *GSI Helmholtzzentrum für Schwerionenforschung GmbH, Planckstrasse 1, D-64291 Darmstadt, Germany*

[6] *Department of Physics, Nara Women's University, Kita-Uoya Nishimachi, Nara, 630-8506 Nara, Japan*

[7] *Department of Life and Environmental Agricultural Sciences, Faculty of Agriculture, Tottori University, 4-101 Koyamacho-Minami, Tottori, 680-8551 Tottori, Japan*

[8] *Center for Nuclear Study, The University of Tokyo, 2-1 Hirosawa, Wako, 351-0198 Saitama, Japan and*

[9] *Stefan Meyer Institute for Subatomic Physics, Austrian Academy of Sciences, Boltzmanngasse 3, A-1090 Vienna, Austria*

(piAF Collaboration)

(Dated: February 28, 2018)

We observed the atomic $1s$ and $2p$ states of π^- bound to ^{121}Sn nuclei as distinct peak structures in the missing mass spectra of the ^{122}Sn$(d,{}^3$He$)$ nuclear reaction. A very intense deuteron beam and a spectrometer with a large angular acceptance let us achieve potential of discovery, which includes capability of determining the angle-dependent cross sections with high statistics. The $2p$ state in a Sn nucleus was observed for the first time. The binding energies and widths of the pionic states are determined and found to be consistent with previous experimental results of other Sn isotopes. The spectrum is measured at finite reaction angles for the first time. The formation cross sections at the reaction angles between 0 and 2° are determined. The observed reaction-angle dependence of each state is reproduced by theoretical calculations. However, the quantitative comparison with our high-precision data reveals a significant discrepancy between the measured and calculated formation cross sections of the pionic $1s$ state.

The spectroscopy of pionic atoms has contributed to the fundamental knowledge of the non-trivial structure of the vacuum in terms of chiral symmetry and quantum chromodynamics (QCD) in the low energy region [1]. The spatial overlaps between the pionic orbitals and the core nuclei peak near the half-density radii of the nuclei. The pions are excellent probes for the study of medium effects in the nuclear matter. An order parameter of the chiral symmetry [2–4], a quark condensate expectation value $\langle\bar{q}q\rangle$, was deduced at the nuclear density in investigations on in-medium modification of an isovector π-nucleon strong interaction through the wave function renormalization [5–10].

The low energy pion-nucleus interaction is described by a phenomenological optical potential. Parameter sets of the potential were obtained by fitting many known pionic-atom and pion-nucleus-scattering data including isotope shifts of pionic atoms with different neutron numbers [8–12]. Among these parameters is an s-wave isovector parameter b_1, which is closely related to the order parameter of the chiral symmetry breaking in the nuclear medium $\langle\bar{q}q\rangle_\rho$ [5]. Low-lying pionic orbitals are located in a close vicinity of the core nuclei for $Z \gtrsim 50$ [13]. This localized distribution is due to integration of the attractive Coulomb potential and the repulsive and absorptive strong interaction potential. Determining the levels and widths of the bound states provides quantum-mechanical information that leads to constraints on the strong interaction. Previous experiments discovered methods of directly populating the low-lying orbitals, analyzed them spectroscopically [14–16], and measured pionic states in Pb and Sn nuclei. The ratio of $\langle\bar{q}q\rangle_\rho$ to the in-vacuum value $\langle\bar{q}q\rangle_0$ was evaluated to be $\langle\bar{q}q\rangle_\rho / \langle\bar{q}q\rangle_0 \sim 67\%$ [6] based on the in-medium modification of the isovector interaction, which is in good agreement with chiral perturbation theories [17].

Measurements of the pionic atom formation cross sections at finite reaction angles provide unprecedented information. This contributes to a better understanding of the pionic-atom formation mechanisms and leads to higher accuracy in deduction of the fundamental quantities. Experimental data at larger reaction angles open

new prospects for the identifications of the quantum numbers corresponding to the structures observed in the spectra. Previously one had merely to rely on the comparison between the measured and theoretical spectral shapes [16]. Up to the present experiment, the formation cross sections were measured only in very limited solid angles around 0°. Meanwhile, theories predict reaction-angle dependence mainly originating from the different momentum transfers in the $(d, {}^3\mathrm{He})$ reactions [18]. Only a small angular dependence is expected from the elementary π^- production cross sections of the $n(d, {}^3\mathrm{He})\pi^-$ reaction [19].

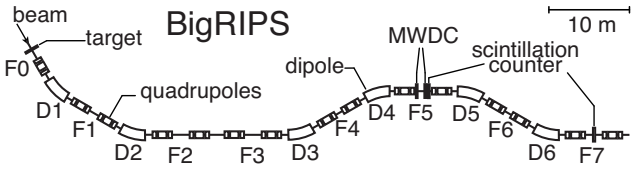

FIG. 1. A schematic view of the experimental facility, BigRIPS [20], and the detector setup. A deuteron beam impinged on a target located at the nominal target position F0. The emitted ^{3}He particles were momentum-analyzed at the dispersive focal plane at F5 and the tracks were measured by the MWDCs. The scintillation counters at F5 and F7 were used for particle identification.

We conducted spectroscopic measurements of the missing mass of the $^{122}\mathrm{Sn}(d, {}^3\mathrm{He})$ nuclear reactions at the RI Beam Factory RIBF, RIKEN [21] in October 2010. The missing mass of the $^{122}\mathrm{Sn}(d, {}^3\mathrm{He})$ reaction near the pion emission threshold was measured for the first time. The experiment demonstrated the excellent performance of RIBF applied in an experimental program of high precision spectroscopy with the primary beam. We employed a deuteron beam with a typical intensity of 2×10^{11}/s accelerated by the cyclotron complex of AVF-RRC-SRC and focused onto the target location of the BigRIPS in-flight magnetic separator [20]. The beam was extracted in micro bunches of frequency of 13.7 MHz and had a high duty factor. The beam energy has been determined to be $T_d = 498.9 \pm 0.2$ MeV by NMR measurements in BigRIPS. The horizontal beam emittance and intrinsic momentum spread have been estimated to be $\sim 0.54 \times 3.0\,\pi$ mm·mrad (σ) and $0.04^{+0.01}_{-0.02}$%, respectively.

Figure 1 illustrates the schematic layout of the employed detectors and BigRIPS used as a spectrometer. The acceptance aperture of $\sim 2°$ was utilized to cover a reaction-angle range centered near 0°. The deuteron beam impinged on a 1 mm wide strip target of ^{122}Sn at F0 which was isotopically enriched to 95.8% and had a thickness of 12.5 ± 0.5 mg/cm^2. The achieved mean luminosities of about 10^{31} cm^{-2} s^{-1} in the present experiment were much higher than those of previous experiments at GSI [6, 14–16] despite of the thinner target. We expected direct formation of pionic atoms coupled with neutron hole states in the nuclear reactions near the recoil-free kinematical condition. Relevant neutron hole states (excitation energies $E_n(n'j'l')$) in the ^{121}Sn nucleus are $2d_{3/2}$ (0.0 MeV), $3s_{1/2}$ (0.06034 MeV), $2d_{5/2}$ (1.1212 MeV), and $2d_{5/2}$ (1.4035 MeV) [22].

The emitted ^{3}He particles were momentum analyzed at F5 with a momentum dispersion of 60.64 ± 0.15 mm/%. We installed two sets of multi-wire drift chambers (MWDC) near the momentum dispersive focal plane at F5 and measured the tracks of the charged particles with a tracking resolution of ~ 40 μm (σ). The ^{3}He ions were identified by the time-of-flight of ~ 174 ns between F5 and F7 measured by the scintillation counters. The counters had a distance of about 23 m. We achieved almost background-free ^{3}He spectra (< 0.1 % contamination). A typical trigger rate of the data acquisition was 200/s due to the relatively narrow coincidence gate between F5 and F7 detectors. The deadtime of the data-acquisition system has been estimated to achieve an efficiency of ~ 93%.

The measured ^{3}He tracks have been used to determine the ^{3}He kinetic energies, the positions, and the angles at the target after detailed analyses and corrections of the optical transfer coefficients up to the fifth order aberrations [23]. Hereafter measured ^{3}He emission angles are treated as the reaction angle θ. The θ resolution has been estimated to be $\sim 0.3°$ (σ). The mass of the reaction product, the pionic atom, has been determined by the measured ^{3}He energy and θ. It has been related to the excitation energy E_{ex} relative to the ground-state mass of ^{121}Sn ($M(^{121}\mathrm{Sn})$). The corresponding relation at 0° is given by the equation $E_{\mathrm{ex}} = [M_{\mathrm{mm}} - M(^{121}\mathrm{Sn})]c^2 = m_{\pi^-}c^2 - B_{nl} + E_{\mathrm{n}}(n'l'j')$ where M_{mm} is the mass of the reaction product, B_{nl} is the binding energy of the pion in a state characterized by the principal (n) and angular (l) quantum numbers. $m_{\pi^-} = 139.571$ MeV/c^2 is the π^- rest mass.

The ^{3}He kinetic energy has been calibrated by using the two-body reaction of $p(d, {}^3\mathrm{He})\pi^0$. The target consists of a 100 ± 1 μm thick 2 mm wide polyethylene strip. We performed a calibration measurement every two hours during the production runs. The calibration spectra have low-energy tails due to the large reaction angles. Therefore, we have examined the spectral response by Monte Carlo simulations including effects of matter, spectrometer acceptance and detector performances. A fit has been conducted to reproduce the entire spectral shape in the plane of the measured positions and angles and related them to the ^{3}He energies. The systematic errors of the absolute E_{ex} values have been estimated to be $^{+0.036}_{-0.033}$ MeV (σ).

The $p(d, {}^3\mathrm{He})\pi^0$ reaction has also been used to calibrate the effective beam intensity on the target. The reaction cross section has been estimated to be 7.6 μb/sr in the θ range of 0 – 0.5° based on an extrapolation of the data at a slightly higher energy to ours [24]. For this

we have used the measured beam energy dependence in Ref. [25]. After applying an acceptance correction of the spectrometer evaluated by a Monte Carlo simulation, we have estimated a systematic error for the absolute cross section scale of 30%.

The experimental resolution has been estimated by the quadratic sum of contributions from the incident beam emittance and intrinsic momentum spread, the target thickness, and the optical aberrations of the spectrometer. We have found a quadratic dependence of the resolution on $E_{\rm ex}$ due to combined effects of multiple scattering at a vacuum window at F5 and higher-order optical-aberrations. This dependence has been estimated to be $R(E_{\rm ex}) = \sqrt{R^2_{\rm min} + (0.122 \times (E_{\rm ex} - 139.799\ {\rm MeV}))^2}({\rm FWHM})$ with the resolution minimum $R_{\rm min} = 0.42$ MeV, which agrees with the measured spectral responses in the calibration reaction of $p(d, {}^3{\rm He})\pi^0$.

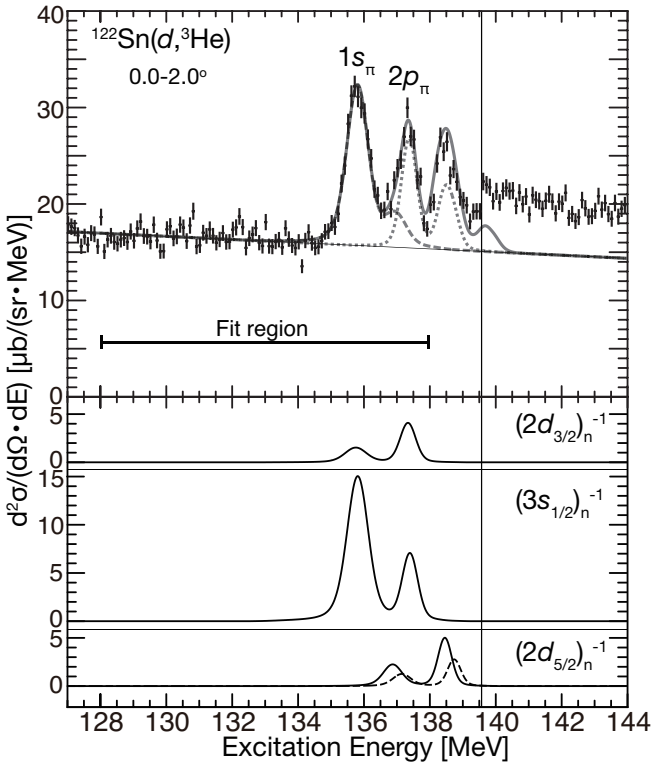

FIG. 2. (Top panel) Measured excitation spectrum of the ^{122}Sn$(d, {}^3{\rm He})$ reaction at the angular range of $0 < \theta < 2°$. Three distinct peaks are observed in the region $E_{\rm ex} =$ [134,139] MeV. The left and middle peaks are mainly originating from formation of pionic $1s$ and $2p$ states, respectively. The right peak is partly contributed from the other pionic states ($2s, 3p$, and $3s$). The spectrum is fitted in the region indicated. The fitting curve and contributions from the $1s$ and the $2p$ states are presented by solid, dashed and dotted lines, respectively. (Bottom panel) Decomposition of the pionic $1s$ and $2p$ strengths into contributions from each neutron hole state of ^{121}Sn as indicated. Note that fragmentation is taken into consideration for $(2d_{5/2})_n^{-1}$.

Figure 2 (top panel) displays the measured excitation spectrum for nearly the full acceptance of the spectrometer. The abscissa is the excitation energy and the ordinate is the double differential cross section of the ^{122}Sn$(d, {}^3{\rm He})$ reaction. The π^- emission threshold is indicated by the vertical solid line at 139.571 MeV. On the left side of the spectrum in the range of $E_{\rm ex} < 134$ MeV, a linear background is observed for nuclear excitation without pion production. Above the emission threshold a continuum is observed due to quasi-free pion production.

Three prominent peaks are observed below the pion emission threshold in the region of 134 MeV $\lesssim E_{\rm ex} \lesssim$ 139 MeV. The leftmost peak is due to the formation of a pionic $1s$ state mainly coupled with a neutron hole state of $(3s_{1/2})_n^{-1}$. The middle peak contains contributions from the configurations $(1s)_\pi(2d_{5/2})_n^{-1}$, $(2p)_\pi(3s_{1/2})_n^{-1}$ and $(2p)_\pi(2d_{3/2})_n^{-1}$. The peak on the right side originates mainly from the $(2s)_\pi(3s_{1/2})_n^{-1}$ and $(2p)_\pi(2d_{5/2})_n^{-1}$ configurations.

The spectrum has been fitted in an excitation energy region [128.0,138.0] MeV with calculated spectra based on theoretical pionic atom formation cross sections in Ref. [26] folded by the experimental resolution expressed by Gaussian functions. Pionic $1s$, $2p$, $2s$, $3p$, and $3s$ states have been taken into considerations and other higher states as well as the quasi-free contributions have been neglected. In the fit 8 parameters have been used: the differential cross sections $(d\sigma/d\Omega)$ of pionic (nl) states I_{1s}, I_{2p}, the binding energies B_{1s}, B_{2p}, the $1s$ width Γ_{1s}, and a slope and an offset for the linear background. The $2p$ width has been fixed to a calculated value of 0.109 MeV [18, 27] since it is much smaller than the experimental resolution. Since contributions from the other states $2s$, $3p$ and $3s$ are small, their binding energies and widths have been fixed to theoretical values and their relative cross section ratios I_{2s}/I_{1s}, I_{3s}/I_{1s} and I_{3p}/I_{2p} to theoretical ratios [18, 27]. The resolution minimum $R_{\rm min}$ has also been used as a free parameter.

The fitted curve is presented with contributions from the pionic $1s$ and $2p$ states. The overall fit has a χ^2/n.d.f of 135.8/92. Figure 2 (bottom panel) shows the decomposition of the $1s$ and $2p$ formation cross sections into different neutron hole states of ^{121}Sn as indicated. The peak on the left is coupled with pionic $1s$ and the one on the right with $2p$.

We have evaluated the systematic errors attributed to the deduced binding energies and width resulting from i) absolute $E_{\rm ex}$ scale error arising from the energy calibration, the uncertainty of the primary beam energy, the uncertainty of the target thickness and the ion-optical properties of the spectrometer, ii) the $E_{\rm ex}$ dependence of the resolution within evaluated errors, iii) the fitting region and iv) 20% errors in the spectroscopic factors of relevant neutron holes. The systematic errors of the binding energies are mainly arising from the energy cali-

bration and the dispersion of the spectrometer.

The binding energies and width are deduced to be

$$B_{1s} = 3.828 \pm 0.013(stat.)^{+0.036}_{-0.033}(syst.)\ \text{MeV}$$
$$\Gamma_{1s} = 0.252 \pm 0.054(stat.)^{+0.053}_{-0.070}(syst.)\ \text{MeV}$$
$$B_{2p} = 2.238 \pm 0.015(stat.)^{+0.046}_{-0.043}(syst.)\ \text{MeV}.$$

with the statistical and systematic errors. The achieved resolution minimum of $R_{\min} = 0.394^{+0.064}_{-0.044}$ MeV is consistent with the estimation of 0.42 MeV described above. B_{1s} and B_{2p} of a pionic Sn isotope are determined simultaneously for the first time. The deduced B_{1s}, Γ_{1s} and B_{2p} fairly well agree with the theoretical values $B^{\text{theo}}_{1s} = 3.787$ – 3.850 MeV, $\Gamma^{\text{theo}}_{1s} = 0.306$ – 0.324 MeV and $B^{\text{theo}}_{2p} = 2.257$ – 2.276 MeV [18, 27].

The measured spectrum has been decomposed into different θ ranges expecting the θ dependence of the formation cross sections [18, 26, 28]. Figure 3 shows the excitation spectra for θ in the ranges of 1.5 – 2.0°, 1.0 – 1.5°, 0.5 – 1.0° and 0 – 0.5°. The peak structures are clearly observed for each θ range. The peak positions and widths are nearly constant for the different θ ranges, which demonstrates the high quality of the measurement.

The decomposed spectra have been fitted to deduce θ-dependent cross sections for the pionic $1s$ and $2p$ states, $I_{1s}(\theta)$ and $I_{2p}(\theta)$, with other parameters fixed to those determined in the fitting procedure described above. The linear background has been scaled by a parameter for each angular range. The resulting fitting curves are shown together with curves for $1s$ and $2p$ contributions.

Figure 4 (top panel) depicts $I_{1s}(\theta)$ (black) and $I_{2p}(\theta)$ (grey). The abscissa is θ represented by the weighted averages of the solid angles. The boxes show the statistical errors and the bars the systematic errors in addition. They have been studied in the same way as those conducted for the binding energies and widths. An overall systematic error of 30% is attributed to the absolute scale of the cross section. The dashed curves show theoretically calculated cross sections of the pionic $1s$ and $2p$ states using phenomenological neutron wave functions of Koura-type given in Ref. [29]. The solid curves show the same but scaled with fitted factors of 0.17 and 0.79 for the $1s$ and $2p$ states, respectively. We observe that the theoretical θ dependences reproduce well the experimental data, which confirms the assignments of the angular momenta of the states. In principle, this suggests that the theoretical models of finite momentum transfer [18] are valid. However, the absolute value of measured $I_{1s}(\theta)$ is much smaller than the theoretical calculation. Figure 4 (bottom panel) shows the ratios of the $I_{2p}(\theta)$ and $I_{1s}(\theta)$. The large discrepancies between the experimental data and the theory suggest missing factors of the formation cross sections which have to be independently applied to the pionic states.

In conclusion, we have performed spectroscopy of pionic ^{121}Sn atoms and observed the $1s$ and $2p$ states as prominent peak structures. For Sn, the $2p$ state is observed as a peak structure for the first time. We have determined the binding energies of the $1s$ and $2p$ states and the width of the $1s$ state. The reaction-angle dependences of the pionic atom formation cross sections are measured and found to agree with the theoretical dependences, which supports the assignments of the quantum-numbers of the measured peak structures. We also find remarkable agreement with theoretically calculated $2p$ formation cross sections over a wide range of reaction

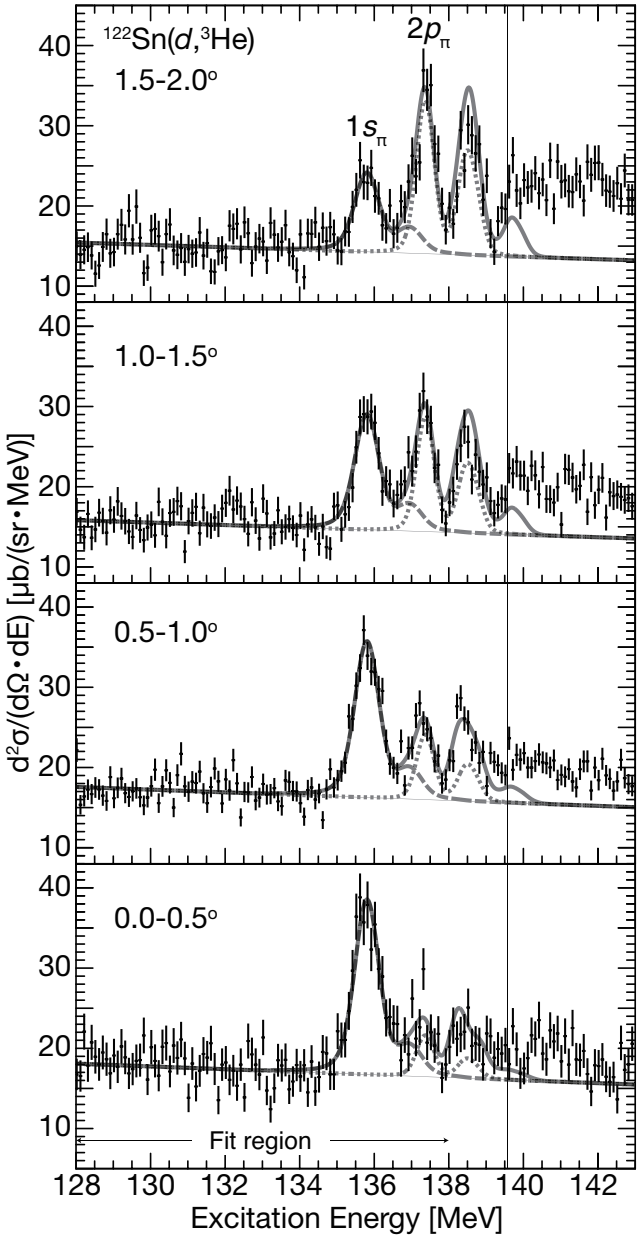

FIG. 3. The measured excitation spectrum in Fig. 2 is decomposed into spectra with different θ ranges as indicated. The overall fitting curves and the $1s$ and $2p$ components are shown by the solid, dashed and dotted lines, respectively.

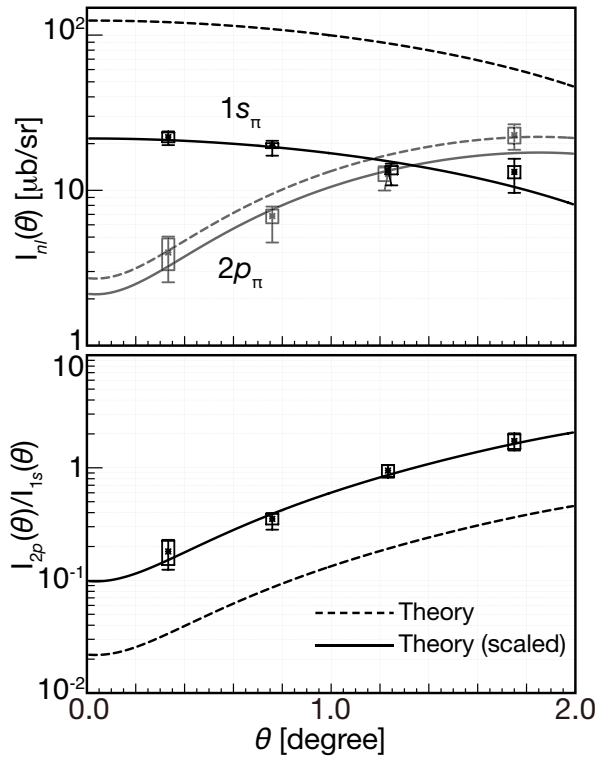

FIG. 4. (Top panel) Determined pionic-nl-state formation cross sections $I_{nl}(\theta)$ for different θ ranges. Statistical errors are shown by the boxes and systematic errors in addition by the bars. The deduced cross sections are compared with the theoretical calculations [18, 27]. (Bottom panel) $I_{2p}(\theta)/I_{1s}(\theta)$. Systematic errors are canceled by taking the ratios.

angles. However, the measured absolute cross sections of the 1s state are smaller by a factor of ~ 5. Note that the entire data were accumulated within 15 h, which is showing the potential of the facility RIBF for spectroscopy experiments. Continuous development is in progress aiming at a better spectral resolution of ≤ 150 keV. The major accomplishments in the present experiment will be succeeded by experiments with improved resolution, statistics and systematics errors to deduce π-nucleus isovector scattering length b_1 with better accuracy [30]. A new series of experiments to study pionic atoms over a wide range of nuclei is in preparation and will lead to a better understanding of the fundamental structure of the QCD vacuum based on measurements.

The authors thank Prof. Emeritus Dr. Toshimitsu Yamazaki for fruitful discussions and late Prof. Emeritus Dr. Paul Kienle for his guidance in this study. The authors are grateful to the staffs of GSI for providing target materials and staffs of RIBF for stable operation of the facility. This experiment was performed at RI Beam Factory operated by RIKEN Nishina Center and CNS, University of Tokyo. This work is partly supported by MEXT Grants-in-Aid for Scientific Research on Innovative Areas (Grants No. JP22105517, No. JP24105712 and No. JP15H00844), JSPS Grants-in-Aid for Scientific Research (B) (Grant No. JP16340083), (A) (Grant No. JP16H02197) and (C) (Grants No. JP20540273 and No. JP24540274), Grant-in-Aid for JSPS Research Fellow (Grant No. 12J08538), the Bundesministerium für Bildung und Forschung, and the National Science Foundation through Grant No. Phys-0758100, and the Joint Institute for Nuclear Astrophysics through Grant No. Phys-0822648 and PHY-1430152 (JINA Center for the Evolution of the Elements).

* Email: itahashi@riken.jp

[1] P. Kienle and T. Yamazaki, Prog. Part. Nucl. Phys. **52**, 85 (2004).
[2] M. Gell-Mann, R. J. Oakes, and B. Renner, Phys. Rev. **175**, 2195 (1968).
[3] Y. Tomozawa, Nuovo Cimento **A 46**, 707 (1966).
[4] S. Weinberg, Phys. Rev. Lett. **17**, 616 (1966).
[5] E. E. Kolomeitsev, N. Kaiser, and W. Weise, Phys. Rev. Lett. **90**, 092501 (2003).
[6] K. Suzuki *et al.*, Phys. Rev. Lett. **92**, 072302 (2004).
[7] R. S. Hayano and T. Hatsuda, Rev. Mod. Phys. **82**, 2949 (2010).
[8] T. Yamazaki *et al.*, Phys. Rept. **514**, 1 (2012).
[9] E. Friedman and A. Gal, Phys. Rept. **452**, 89 (2007).
[10] E. Friedman and A. Gal, Nucl. Phys. **A 928**, 128 (2014).
[11] C. J. Batty, E. Friedman, and A. Gal, Phys. Rept. **287**, 385 (1997).
[12] J. Konijn *et al.*, Nucl. Phys. **A 519**, 773 (1990).
[13] H. Toki *et al.*, Nucl. Phys. **A 501**, 653 (1989).
[14] T. Yamazaki *et al.*, Z. Phys. A **355**, 219 (1996).
[15] H. Gilg *et al.*, Phys. Rev. **C 62**, 025201 (2000).
[16] K. Itahashi *et al.*, Phys. Rev. **62**, 025202 (2000).
[17] U.-G. Meissner, J. A. Oller, and A. Wirzba, Ann. Phys. (N.Y.) **297**, 27 (2002), and references therein.
[18] N. Ikeno *et al.*, PTEP **2015**, 033D01 (2015).
[19] W. J. Frank *et al.*, Phys. Rev. **94**, 1716 (1954).
[20] T. Kubo, Nucl. Instr. Meth. Phys. Res. **B 204**, 97 (2003).
[21] Y. Yano, Nucl. Instr. Meth. Phys. Res. **B 261**, 1009 (2007).
[22] S. Ohya, Nucl. Data Sheets **111**, 1619 (2010).
[23] T. Nishi *et al.*, Nucl. Instr. Meth. Phys. Res. **B 317**, 290 (2013).
[24] K. R. Chapman *et al.*, Nucl. Phys. **57**, 499 (1964).
[25] M. Betigeri *et al.*, Nucl. Phys. **A 690**, 473 (2001).
[26] N. Ikeno *et al.*, Prog. Theor. Phys. **126**, 483 (2011).
[27] N. Ikeno and T. Nishi, *private communication* (2017).
[28] N. Ikeno, H. Nagahiro and S. Hirenzaki, Euro. Phys. J. **A 47**, 161 (2011).
[29] H. Koura and M. Yamada, Nucl. Phys. **A 671**, 96 (2000).
[30] K. Itahashi *et al.*, RIBF Proposal **054R1** (unpublished) (2013).